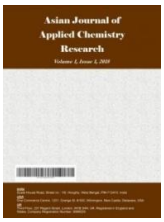

Asian Journal of Applied Chemistry Research

3(1): 1-16, 2019; Article no.AJACR.48832

Effect of Metal on the Properties of the Azopyridine Complexes of Iron, Ruthenium and Osmium

Ouattara Wawohinlin Patrice[1], Bamba Kafoumba[1*], N'guessan Nobel Kouakou[1] Koné Mamadou Guy Richard[1], Kodjo Charles Guillaume[1] and Nahosse Ziao[1]

[1]Laboratoire de Thermodynamique et Physico-Chimie du Milieu, Université Nangui Abrogoua, Côte d'Ivoire.

Authors' contributions

This work was carried out in collaboration among all authors. Author OWP designed the study, performed the statistical analysis, wrote the protocol and wrote the first draft of the manuscript. Authors BK and NNK managed the analyses of the study. Authors KMGR, KGC and NZ managed the literature searches. All authors read and approved the final manuscript.

Article Information

DOI: 10.9734/AJACR/2019/v3i130084
Editor(s):
(1) Dr. Angélica Machi Lazarin, Professor, Department of Chemistry, State University of Maringá, Brazil.
Reviewers:
(1) Gühergül Uluçam, Trakya University, Turkey.
(2) Dolunay Sakar Dasdan, Yildiz Technical University, Turkey.
(3) Saturnino Carmela, University of Basilicata, Potenza, Italy.
(4) Fatma Kandemirli, Kastamonu University, Turkey.
Complete Peer review History: http://www.sdiarticle3.com/review-history/48832

Original Research Article

Received 24 February 2019
Accepted 03 May 2019
Published 10 May 2019

ABSTRACT

The theoretical study of α-, β-, γ-, δ-, ε- $MCl_2(Azpy)_2$ isomers with (M = Fe, Os and Ru) complexes is carried out using Density Functional Theory (DFT) at the B3LYP / LANL2DZ level. This study is focused not only on the effect of metals over geometric, electronic and reactivity parameters, but also on their anti-cancer effect. Its results that the geometric parameters undergo small modifications. These modifications evolve from iron to osmium through ruthenium complexes. Thus, the lengths of the bonds M-X (with X = Cl, N_2, N_{py}) follow the following order Fe-X <Ru-X <Os-X. However, regarding their angular variation that undergoes deformation through the octahedron shape, it could be related to Jahn Teller effect. Also, the substitution of Ru by Os would increase the reactivity of these complexes. Among the isomers studied, the ε-Fe, δ-Ru and δ-Os complexes are likely to bind easily to the DNA. The values of the dipole moments are arranged in the following order: μ (ε-M)> μ (β-M)> μ (α-M)> μ (γ-M)> μ (δ-M) within these azopyridine

**Corresponding author: Email: bambakaf.sfa@univ-na.ci;*

complexes. Finally, we notice that the substitution of Ru by Os improves the cytotoxicity and the fluorescence of these complexes. The δ-Os isomer has the best cytotoxic and photosensitive characteristics of these azopyridine complexes and would be the ideal isomer for the diagnosis and treatment of cancers.

Keywords: Cancer; azopyridine; fluorescence; DFT; TDDFT; iron; ruthenium; osmium.

1. INTRODUCTION

The cancer remains today one of the most dangerous diseases to be eradicated despite the improvement in its detection, its prevention and its treatment. Some cancers can be caused by smoking, obesity, physical inactivity and infections [1]. Several treatment methods such as chemotherapy exist, yet they have many failures that can sometimes be related to metastases and side effects. Therefore, current research focuses on methods or drugs that combine efficacy and low side effects. Since the successful development of cis-$[PtCl_2(NH_3)_2]$ (cisplatin) [2] as a cancer drug, many efforts are based on the development of transition metal-based drugs thanks to their high clinical efficacy, the reduction of systemic toxicity and the prolonged multiple activity in which cisplatin is even totally inactive. The low oxidation states Ru (II) or Ru (III) compounds are considered suitable candidates for the implementation of anticancer drugs, since the kinetics of the substitution reactions of their ligands is like those of platinum (II) compounds. Some of these drugs have been shown to be highly effective against metastases of solid tumors in both experimental tumors and human tumors grafted in nude mice [3, 4]. Since then, azopyridine Ru (II) complex is the subject of intense research.

Azopyridines ligands are organic compounds consisting of a pyridine group and an aromatic ring, linked together by an azo bond N=N. The electron-rich azo group (-N=N-) gives some rigidity to the azopyridine ligand. The arylazopyridine complexes of Ru (II), $Ru(Azpy)_2Cl_2$ where Azpy stands for 2-phenylazopyridine, represent a class of well-characterized anticancer compounds. There are five well known different isomers of these complexes owing to the unsymmetry of the ligand [5]. Their activity has a strong structural dependence [6]. Reedijk et al. reported that the elevated cytotoxicity of α and γ isomers in vitro (A498, EVSA-T, H226, IGROV, MCF-7, WIDR, M19 cells) were compared to cisplatin and 5-fluorouracil, which are approximately 10 times higher than the corresponding β isomer [7]. Modifications have been made to these isomers to improve their cytotoxic characteristics. However, the addition of methyl groups to the pyridine or phenyl ring, giving respectively $Ru(tazpy)_2Cl_2$ and $Ru(mazpy)_2Cl_2$ (tazpy = o-tolylazopyridine and mazpy = 4-methyl-2-phenylazopyridine) did not alter the rank of cytotoxicity given by the SAR (structure-activity relationship) study over the starting isomers. Other modifications have been undertaken to improve the solubility of these azopyridine complexes. For instance, water-soluble derivatives of the α-isoform where the chloride ligands are replaced by nitrate, 1,1-cyclobutanedicarboxylate, oxalate or malonate ligands have been developed but all these complexes were found less cytotoxic than the α isomer (A2780, A2780cisR). Nevertheless, their activity remains comparable to carboplatin's [8]. The structural characteristics of these compounds have a significant impact on the effectiveness of cytotoxic compounds.

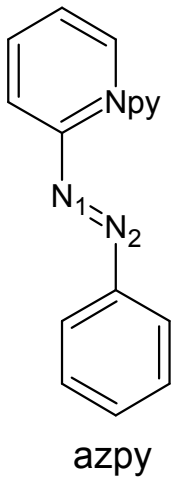

azpy

Fig. 1. Ligand Azpy with three nitrogen atoms and the ligand is assumed to bind the metal by both N_2 and N_{py} as to highlight its bidentate state. This ligand is used to form a ring of five atoms with the metal

In a recent work, we studied the effect of halogen atoms on the activity of $RuX_2(Azpy)_2$ where X

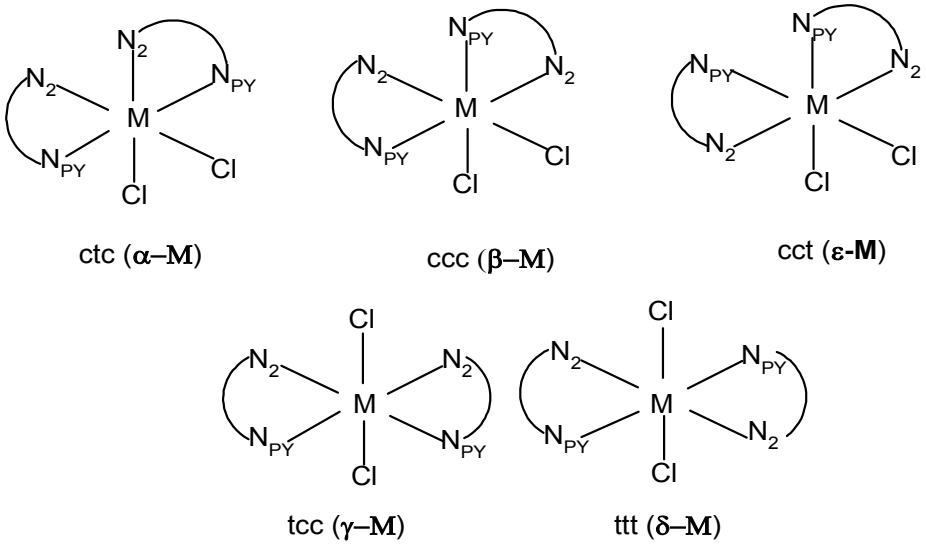

Fig. 2. The five isomers likely to form with the azopyridine ligand. All these isomers are of C_2 symmetry except the β isomer. Here, α-M, β-M and ε-M are the cis complexes while γ-M and δ-M represent both the trans isomers

stands for F, Cl, Br and I. we showed that the strength of activity of the complex evolves according to electronegativity of halide atoms. Thus, complexes $RuF_2(Azpy)_2$ were discovered to be the most active molecules [9].

Here, we want to evaluate by means of theoretical tools, the effect of certain metals on the anti-cancer properties of azopyridine complexes. The metals chosen are Fe, Ru and Os. Their common particularity is that they belong to the same group of the periodic table. Hence, they must form the same number of isomers. Moreover, the ligand chosen for the complexation of these metals remains the well-studied 2-phenylazopyridine which structure is displayed in Fig. 1.

According to previous papers, we showed that five complexes are always formed between Azpy ligand and any metal atom as illustrated in the Fig. 2 [5]. These isomers are formed according to the following reaction:

$$MCl_3, 3H_2O + 2L \rightarrow MCl_2L_2 + ½\ Cl_2 + 3H_2O$$

Where,

M =Fe, Ru
Os and L =Azpy

2. METHODS OF CALCULATIONS

2.1 DFT Calculations

The optimization of the molecules was carried out in the gas phase using GAUSSIAN 09 software [10]. The minimal energy structure was performed using density functional theory (DFT). All DFT calculations were performed using the Becke B3LYP 3-parameter hybrid functional [11, 12, 13, 14] and the basis set containing the double zeta pseudo-potential Lanl2DZ [15, 16]. Today, the DFT method allows to clarify many chemical phenomena in a wide variety of fields that encompasses energy production (photovoltaic, fuel cells, nuclear), geochemistry (minerals, the earth's core) and biology (enzymes, proteins, DNA). In the latter field for example, the study of enzymatic catalysis, has allowed the rationalization of experimental data and the elucidation of reaction mechanisms for many enzymes [16]. The geometry optimizations were performed at fundamental states of these complexes and they were assumed to be in a singulet state [17]. In addition, the stable configuration of the isomers was confirmed by frequency analysis in which no imaginary data was observed for all minimum energy configurations. Therefore, DFT methods with B3LYP and Lanl2dz basis set are assumed so

far to be consistent with experiment data performed on ruthenium complexes [13]. The energy of Frontier molecular orbitals (HOMO and LUMO) were analyzed. The analysis of the natural orbital population NPA was also carried out.

2.2 Spectral Constant

The excitation of a molecule or an atom without an external magnetic field during an average time $\tau = 1{,}499/f.E^2$ can allow a photo emission [18]. Here f represents the oscillation force of the transition and E the wavenumber of excitation expressed in cm^{-1}. τ represents the life time of the excited state. Besides, the coefficients probability of Einstein's transition given by A_{if} for emission and B_{if} for absorption between the initial (i) and final (f) electronic states are given as follows [19]:

$$A_{if} = 1 / \tau$$

where τ is the life time expressed in seconds.

$$B_{if} = 14{,}50.10^{24}\, D_{if}$$

where D_{ij} is the dipole moment of transition. In general, the dipole moment of transition can be obtained by the following relation:

$D_{ij} = 4{,}24.10^{-20}.\frac{c\hbar}{v}\,\varepsilon_{max,}$ where $\hbar$ is the half-width of the absorption band in cm^{-1}, ε_{max} the molar extinction coefficient and c the speed of light, 3×10^{10} cm s^{-1}, v the radiation frequency in s. Specific indices of reactivity [20, 21] have been established according to the following relationships:

- chemical potential $\mu = (\varepsilon(HOMO) + \varepsilon(LUMO)) / 2$,
- the absolute chemical hardness $\eta = (\varepsilon(LUMO) - \varepsilon(HOMO)) / 2$,
- electrophilia $\omega = \mu^2 / 2\eta$,
- nucleophilia $N = \varepsilon HOMO\,(Nu) - \varepsilon HOMO\,(TCE)$, where tetracyanoethylene (TCE) is the reference because it has the lowest energy of the HOMO among the series of molecules already explored in the context of organic polar reactions [19].

3. RESULTS AND DISCUSSION

3.1 The Geometrical Parameters

The geometrical parameters regard the metallic bonds that are assumed to influence the shape of the molecules. Those bonds are M-Cl, M-N_2 and M-N_{Py}. Both chloride atoms have sometime different bonding to the metal. So, they are numbered to emphasize the difference between both bondings that can be at the origin of a symmetry. Besides, the distance between the two nitrogen atoms within the ligand forming the azo group (N=N) which confers a certain rigidity to the ligand can also undergo a modification. Moreover, several angles formed with the metal like Cl_1-M-Cl_2, N_{py}-M-N_{py} and N_2-M-N_2 vary from a molecule to another. Table 1 display these geometrical parameters.

In general, the bond's lengths undergo a variation which depends on the nature of the metal atom. Since all metal belong to the same group in the periodic table, the lengths M-X with M = Fe, Ru, Os and X = Cl, N_2, N_{Py} such as M-Cl, M-N_2 and M-N_{Py} follow the same trends depending on the metallic shape. Indeed, the lengths MX increase from Fe to Os atoms. Therefore, we have the following classifications: Fe-Cl <Ru-Cl <Os-Cl; Fe-N_2 <Ru-N_2 <Os-N_2 and Fe-N_{Py} < Ru-N_{Py} < Os-N_{Py}. Likewise, the bonding of the azo group follows the same order with Fe(N=N) < Ru (N=N) < Os (N=N). From this analysis, we can conclude that the metallic substitution triggers an elongation of the distance between the metal atom and the atoms directly linked to it. This elongation within these complexes is certainly due to the electronegativity of metal atoms [22]. According to the Pauling scale, the electronegativities of these metal atoms are 1.83 and 2.2 respectively for iron and for both ruthenium and osmium. Here, the identical electronegativity of both Ru and Os atoms explains the proximicity of theirs bondings in the complexes. Moreover, it is found that the values obtained theoretically and experimentally regarding Ru isomers are in good agreement. Furthermore, we notice that the metal has no influence on the deformation of the octahedral structure of these complexes in sofar that the Cl_1-M-Cl_2 angle remains the same for all the δ-M isomers. The particularity of this isomer is that both Cl atoms are different. Also, it has a C_2 axis of symmetry that passes through the two chlorine and the metal atoms. Therefore, we assume that this configuration reduces Coulomb repulsions due to the high electronegativity of the chlorine atoms which is 3.16 according to the Pauling scale. Regarding the other isomers such as α-M, γ-M and ε-M, they also have a C_2 axis of symmetry, but this axis does not pass through the two chlorine atoms and the metal atom. Moreover, they have all their atoms identical by

pair thereby justifying their C_2 symmetry. Whereas the β-M isomer, it has no C_2 axis of symmetry and all atoms are different. Yet, all five isomers display a deformation of the octahedron. Therefore, the octahedral deformation of these complexes must certainly be caused by Jahn Teller effect [23] through which frontier orbitals degenerate for the complexes' stabilizations. it results from that analysis that whatever the nature of the metal, Azpy ligand imposes the structure of the complex.

Table 1. Geometric parameters of Azpy complexes at B3LYP / LANLD2Z level; lengths are set in (Å) and angles are in (°)

		$N_1=N_2$	M-N_2	M-N_{py}	M-Cl_1	M-Cl_2	Cl_1-M-Cl_2	N_{py}-M-N_{py}	N_2-M -N_2
α- Fe	Calc	1.31	1.94	1.96	2.39	2.39	92.58	177.76	100.31
β- Fe	Calc	1.31-1.31	1.98-1.95	1.96-1.97	2.39	2.39	93.59	96.23	104.16
γ- Fe	Calc	1.30	1.99	1.98	2.39	2.39	176.12	103.87	98.18
δ- Fe	Calc	1.30	1.98	2.01	2.40	2.40	180.00	166.73	171.24
ε-Fe	Calc	1.31	1.96	1.97	2.39	2.39	96.98	90.25	172.35
α-Ru	Calc	1.32	2.03	2.06	2.48	2.48	90.58	178.37	101.51
	Exp	1.28	2.03	2.05	2.40	2.40	89.50	174.50	93.50
β-Ru	Calc	1.32-1.32	2.02-2.05	2.05-2.07	2.48	2.48	90.18	99.21	104.58
	Exp	1.29-1.30	1.96-2.00	2.02-2.06	2.40	2.41	91.10	101.90	103.00
γ-Ru	Calc	1.32	2.03	2.10	2.48	2.48	170.71	102.86	104.99
	Exp	1.31	1.99	2.11	2.38	2.38	170.50	103.80	104.10
δ-Ru	Calc	1.31	2.06	2.10	2.49	2.51	180.00	167.53	178.58
	Exp	1.28	2.02	2.06	2.38	2.38	180.00	180.00	180.00
ε-Ru	Calc	1.32	2.05	2.06	2.49	2.49	94.10	93.58	169.48
α-Os	Calc	1.34	2.00	2.05	2.48	2.48	88.36	178.92	101.43
β-Os	Calc	1.34–1.34	2.02-1.99	2.07-2.04	2.47	2.48	87.84	99.64	103.56
γ-Os	Calc	1.34	2.00	2.10	2.47	2.47	166.67	103.95	104.49
δ-Os	Calc	1.32	2.03	2.08	2.50	2.50	180.00	169.42	175.25
ε-Os	Calc	1.34	2.03	2.05	2.48	2.48	91.24	168.64	96.17

Table 2. Global reactivity parameters: Frontier molecular orbitals HOMO and LUMO, energy gap and free enthalpy reaction in Kcal.mol^{-1} at B3LYP/LANLD2Z level

Isomers	E_{HOMO}	E_{LUMO}	ΔE_{L-H}	ΔG°
α-Fe	-5,633	-3,276	2,357	6,360
β-Fe	-5,523	-3,276	2,247	10,330
γ-Fe	-5,648	-3,279	2,369	14,470
δ-Fe	-5,588	-3,277	2,311	11,680
ε-Fe	-5,554	-3,352	2,202	11,110
α-Ru	-5,553	-3,332	2,221	-16,520
β-Ru	-5,525	-3,224	2,301	-13,330
γ-Ru	-5,385	-3,366	2,019	-8,530
δ-Ru	-5,229	-3,431	1,798	-9,640
ε-Ru	-5,403	-3,362	2,041	-10,410
α-Os	-5,572	-3,306	2,266	-38,090
β-Os	-5,547	-3,151	2,396	-34,930
γ-Os	-5,335	-3,350	1,985	-27,780
δ-Os	-5,074	-3,426	1,648	-24,800
ε-Os	-5,395	-3,255	2,140	-30,240

3.2 Electronic Structure Parameters and Reactivity

3.2.1 Free enthalpy and frontier molecular orbital analysis

Table 2 displays the frontier molecular orbitals HOMO (the highest occupied molecular orbital) and LUMO (lowest unoccupied molecular orbital), the energetic gap and the free enthalpy of reaction. These parameters are specifically known to indicate the global reactivity of molecules. Besides, HOMO and LUMO orbitals are determining parameters in the field of quantum chemistry [24]. They define the electron density at the boundaries for the prediction of the most reactive positions in π electron systems. They determine the ability of the molecule to interact with other molecules. The HOMO energy determines the molecule's ability to donate electrons while the LUMO energy evaluates the ability for the molecule to accept electrons [25, 26, 27, 28]. The gap energy is also used to characterize the chemical reactivity and the kinetic stability of the molecule. A molecule with a weak gap is more polarizable and generally it is associated with a high chemical reactivity including a low kinetic stability and it is also called a soft molecule [5]. Molecules possessing a conjugation system are characterized by a low value of the electronic gap energy. The gap also reflects the level of charge transfer between the electron-donor group and the electron-acceptor group via the conjugation within the molecule. The thermodynamic values ΔG° describes the stability of these azopyridine complexes.

Through ΔG°, we can assume that the synthesis of these complexes is spontaneous at room temperature under 1 atmosphere except for Fe where the synthesis requires an energy to be provided for all its isomers owing to the positive values of ΔG°. Moreover, Os complexes are assumed to be the most stable due to their lowest values of ΔG°. In the same trend, the least stable complexes are Fe complexes with the highest values of ΔG°. Therefore, it results from this analysis regarding the stability that it increases downwardly from Fe to Os in respect of the periodic table. Hence, the stability of the complex increases with the shape of the metal. Moreover, we can notice particularly that the most stable complex regarding each metallic atom is α-M isomer.

Regarding the gap energy, Table 2 shows that the most chemically stable isomers are ε-Fe, δ-Ru and δ-Os. These isomers are noticed to be also the most polar and the most kinetically stable. Besides, δ-Os is assumed to be the most candidate as photosensitizer. Furthermore, the electronic interaction of these complexes with other molecules can be two forms: either these complexes will act as nucleophiles, or they will act as electrophiles. In the case of a nucleophilic reaction, the reactivity of these complexes will be evaluated from the HOMO energies of these complexes and the most active will be that will have the highest HOMO energy. In the case of an electrophilic reaction, the reactivities of these complexes will be evaluated from the LUMOs of these complexes and the most active will be that having the lowest LUMO energy. In general, the reactivity of these complexes increases downward in the period. In order to evaluate the activities of these complexes, we have established their order of magnitude in Table 3.

Table 3 indicates that for a nucleophilic reaction of these complexes, the most active complexes are β-Fe, δ-Ru and δ-Os isomers. However, regarding the electrophilic reactions, the most active complexes are ε-Fe, δ-Ru and δ-Os isomers. For Ru and Os complexes anyway, we can see that δ-M represent both the nucleophile and the electrophile confirming the gap energy classification. However, concerning Fe, there is no real stability. From this analysis, we can say that the metallic substitution within the azopyridine complexes modifies their reactivity. Besides, the substitution of Ru by Os increases the reactivity of these complexes.

Table 3. Order of magnitude of the energies of the HOMO and LUMO orbitals of the azpy complexes

Frontier orbitals	Order of energy
HOMO	E_{HOMO} (γ- Fe)< E_{HOMO} (α- Fe)< E_{HOMO} (δ- Fe)< E_{HOMO} (ε- Fe)< E_{HOMO} (β- Fe)
	E_{HOMO} (α- Ru)< E_{HOMO} (β- Ru)< E_{HOMO} (ε- Ru)< E_{HOMO} (γ- Ru)< E_{HOMO} (δ- Ru)
	E_{HOMO} (α- Os)< E_{HOMO} (β- Os)< E_{HOMO} (ε- Os)< E_{HOMO} (γ- Os)< E_{HOMO} (δ- Os)
LUMO	E_{LUMO} (ε- Fe)< E_{LUMO} (γ- Fe)< E_{LUMO} (δ- Fe)< E_{LUMO} (α- Fe)< E_{LUMO} (β- Fe)
	E_{LUMO} (δ- Ru)< E_{LUMO} (γ- Ru)< E_{LUMO} (ε- Ru)< E_{LUMO} (α- Ru)< E_{LUMO} (β- Ru)
	E_{LUMO} (δ- Os)< E_{LUMO} (γ- Os)< E_{LUMO} (α- Os)< E_{LUMO} (ε- Os)< E_{LUMO} (β- Os)

Table 4. Dipolar momentum of the azopyridine complexes

Isomers	Dipole moment			
	x	y	z	Total
α- Fe	0,00	0,00	-7,42	7,42
β- Fe	-2,80	1,77	8,61	9 ,22
γ- Fe	0,00	0,00	1,92	1,92
δ- Fe	0,00	0,00	1,28	1,28
ε- Fe	0,00	0,00	-10,04	10,04
α- Ru	0,00	0,00	-7,26	7,26
β- Ru	-1,74	0,97	8,60	8,83
γ- Ru	0,00	0,00	1,68	1,68
δ- Ru	0,00	0,00	-1,33	1,33
ε- Ru	0,00	0,00	-10,02	10,02
α- Os	0,00	0,00	-6,53	6,53
β- Os	-1,48	0,59	7,94	8,10
γ- Os	0,00	0,00	1,78	1,78
δ- Os	0,00	0,00	-0,79	0,79
ε- Os	0,00	0,00	-9,09	9,09

Table 5. Natural charges of the metal atoms (M = Fe, Ru and Os), Cl atoms and azopyridine ligands of complexes at B3LYP/LanlD2Z level

Isomers	Total natural charge		
	M	Ligand	Cl
α-Fe	-0.02	0.84	-0.82
β-Fe	-0.01	0.83	-0.82
γ-Fe	0.01	0.83	-0.84
δ-Fe	0.04	0.82	-0.86
ε-Fe	-0.01	0.85	-0.84
α-Ru	0.01	0.71	-0.72
β-Ru	0.01	0.71	-0.72
γ-Ru	-0.02	0.76	-0.74
δ-Ru	-0.01	0.79	-0.78
ε-Ru	0.02	0.76	-0.78
α-Os	0.20	0.46	-0.66
β-Os	0.20	0.44	-0.64
γ-Os	0.16	0.44	-0.6
δ-Os	0.16	0.55	-0.71
ε- Os	0.20	0.50	-0.70

3.2.2 Dipole moment

The measurement of the ability of a molecule in chemistry to interact with the water molecules through hydrophilicity is determined by the log P value. In fact, the value of Log P expresses the solubility of the compound in an organic solvent or in water. The hydrophilic notion can be evaluated by the dipole moment. In fact, the dipole moment indicates the solubility force in water of a molecule. Accordingly, a high value of this dipole moment implies only low solubility in an organic solvent and high solubility in water. In fact, the most effective drugs are fat-soluble because many anti-metastatic drugs work in organic solvents [5]. Thus, the table presents the dipole moments of the isomers of Fe, Ru and Os azopyridine complexes.

Table 4 contains the dipole moments of the isomers of each metal complex. We can notice that the values of these dipole moments are arranged for each group of isomers in the following order: μ (ε-M)> μ (β-M)>μ (α-M)>μ (γ-M)>μ (δ-M) within the azopyridine complex. Hence, we can retain that the order of solubility of these isomers does not depend on the nature of the metal atom, but it depends on all the structure. Therefore, the most soluble isomers in organic solvents are those where both chloride atoms are in *trans* position. However, when it comes to compare each isomer of the three metals, the solubility increases as usual from Fe to Os and specifically, the most soluble is assumed to be the δ-Os isomer. Whereas for the aqueous solvents, the ε-Cl isomers present the greatest values regarding their solubility therein. This solubility also decreases from Fe to Os. Furthermore, the isomers having the chlorine atoms in the *trans* position (γ-M and δ-M) are more active in organic medium than those which have the chlorine atoms in the *cis* position (α-M, β-M and ε-M). Thus, it results that osmium increases the cytotoxicity of the complex irrespective of the isomer.

Table 6. Specific indices of reactivity of azopyridine complexes in kcal.mol^{-1}

Isomer	μ	η	ω	N
α-Fe	-4.45	1.18	8.42	3.75
β-Fe	-4.40	1.12	8.61	3.86
γ-Fe	-4.46	1.18	8.41	3.73
δ-Fe	-4.43	1.16	8.50	3.79
ε-Fe	-4.45	1.10	9.01	3.83
α-Ru	-4.44	1.11	8.89	3.83
β-Ru	-4.37	1.15	8.32	3.85
γ-Ru	-4.38	1.01	9.48	3.99
δ-Ru	-4.33	0.90	10.43	4.15
ε-Ru	-4.38	1.02	9.41	3.98
α-Os	-4.44	1.13	8.70	3.81
β-Os	-4.35	1.20	7.89	3.83
γ-Os	-4.34	0.99	9.50	4.04
δ-Os	-4.25	0.82	10.96	4.31
ε-Os	-4.33	1.07	8.74	3.98
Cancer cell	-9.02	2.53	16.07	-2.18

Table 7. Border orbitals with their percentage composition, energy (kcal.mol^{-1}), maximum wavelength (nm), oscillation force, life time of the main transitions of these complexes

Isomers	HOMO(%)	LUMO(%)	ΔE (kcal.mol^{-1})	λ_{max} (nm)	f(L.M^{-1}.cm^{-1})	τ (ns)	Main transition
α-Fe	Fe (42)	L (95)	2.76	449.96	0.062	48.79	$HOMO_5 \rightarrow$ LUMO (77%)
			1.80	687.32	0.026	48.95	$HOMO_1 \rightarrow LUMO_{+1}$ (73%)
β-Fe	Fe (25)	L (91)	2.70	460.25	0.042	61.37	$HOMO_6 \rightarrow$ LUMO (72%)
			1.67	743.51	0.019	75.61	$HOMO_2 \rightarrow$ LUMO (76%)
γ-Fe	Fe (52)	L (99)	2.99	414.27	0.091	30.95	$HOMO_8 \rightarrow$ LUMO (75%)
			1.60	773.62	0.028	28.27	$HOMO_1 \rightarrow$LUMO (81%)
δ-Fe	Fe (40)	L (100)	2.86	433.01	0.068	49.75	$HOMO_7 \rightarrow$ LUMO (90%)
			1.53	812.62	0.023	41.33	$HOMO_1 \rightarrow$ LUMO (92%)
ε-Fe	Fe (40)	L (97)	2.61	474.51	0.044	61.42	HOMO $\rightarrow$ LUMO (90%)
			1.49	833.87	0.016	76.71	$HOMO_1 \rightarrow$ LUMO (87%)
α-Ru	Ru (46)	L (89)	2.92	424.41	0.070	48.32	$HOMO_5 \rightarrow LUMO_{+1}$ (41%)
			1.94	640.38	0.056	38.57	$HOMO_1 \rightarrow LUMO_{+}$1 (51%)
β-Ru	Ru (45)	L (86)	3.20	387.86	0.097	23.19	$HOMO_8 \rightarrow$LUMO (53%)
			1.85	671.17	0.038	23.25	$HOMO_1 \rightarrow$LUMO (84%)
γ-Ru	Ru (54)	L (93)	2.64	469.74	0.124	26.67	$HOMO_3 \rightarrow$LUMO (87%)
			2.04	607.07	0.096	26.68	$HOMO_2 \rightarrow$LUMO (79%)
δ-Ru	Ru (62)	L (98)	3.15	393.22	0.161	14.42	$HOMO_7 \rightarrow$LUMO (70%)
			1.51	821.66	0.059	14.40	$HOMO_5 \rightarrow$LUMO (77%)
ε-Ru	Ru (52)	L (90)	2.86	433.92	0.052	54.17	$HOMO_7 \rightarrow$ LUMO (71%)
			1.71	726.85	0.045	54.28	$HOMO_2 \rightarrow$ LUMO (59%)
α-Os	Os (50)	L (83)	3.35	370.25	0.092	22.32	$HOMO_4 \rightarrow LUMO_{+1}$ (65%)
			2.27	545.86	0.121	36.91	$HOMO_1 \rightarrow LUMO_{+1}$ (45%)
β-Os	Os (25)	L (91)	3.41	363.92	0.140	14.15	$HOMO_9 \rightarrow$ LUMO (58%)
			2.24	552.30	0.115	14.18	$HOMO_2 \rightarrow LUMO_{+1}$ (77%)
γ-Os	Os (46)	L (84)	2.63	470.68	0.167	19.95	$HOMO_3 \rightarrow$ LUMO (83%)
			2.22	557.80	0.221	21.11	$HOMO_2 \rightarrow$ LUMO (48%)
δ-Os	Os (63)	L (91)	3.24	382.32	0.136	16.14	$HOMO_9 \rightarrow$ LUMO (83%)
			1.65	753.36	0.064	16.17	$HOMO_1 \rightarrow$ LUMO (74%)
ε-Os	Os (56)	L (83)	3.19	389.09	0.111	20.40	$HOMO_8 \rightarrow$LUMO (90%)
			2.09	592.36	0.094	20.53	$HOMO_2 \rightarrow$LUMO (52%)

Table 8. Contribution as a percentage of M = Fe, Ru, Os, Azpy and chlorine ligands in the OM_i orbitals (initial orbital) and OM_j (final orbital) of the main transitions of these complexes

	Transitions de type π→π* ; OM_i→OM_j						Transitions de type t_{2g}→π*; OM_i → OMj					
	Composition OM_i			Composition OM_j			Composition OM_i			Composition OM_j		
Complexes	**M%**	**Cl%**	**Azpy%**	**M%**	**Cl%**	**Azpy%**	**M%**	**Cl%**	**Azpy%**	**M%**	**Cl%**	**Azpy%**
α-Fe	22	56	22	5	2	93	3	88	9	14	2	84
β-Fe	37	43	20	9	2	89	25	66	10	29	2	90
γ-Fe	29	23	48	1	4	95	42	49	9	1	4	95
δ-Fe	37	35	28	0	5	95	51	41	8	0	4	96
ε-Fe	41	36	23	3	3	94	28	56	16	3	3	94
α-Ru	26	41	33	21	3	76	45	34	21	21	3	76
β-Ru	23	25	52	14	2	84	32	46	23	17	3	80
γ-Ru	1	82	17	7	4	89	74	3	23	7	4	89
δ-Ru	23	36	41	2	3	95	39	40	21	2	3	95
ε-Ru	22	27	51	10	1	89	26	48	26	10	1	89
α-Os	2	19	79	27	4	69	46	20	34	27	4	69
β-Os	37	20	43	9	1	90	36	31	33	23	4	74
γ-Os	1	8	91	16	6	78	69	26	29	16	6	78
δ-Os	12	41	47	9	3	88	36	31	33	9	3	88
ε-Os	2	0	98	17	2	81	29	36	34	17	1	82

OM_i= initial orbital of transition *OM_j= final orbital of transition*

3.2.3 Atomic net charge

To study the metal-ligand interactions in all isomers of the $FeCl_2(Azpy)_2$, $RuCl_2(Azpy)_2$ and $OsCl_2(Azpy)_2$ complexes, we used the NBO analysis method. This analysis was performed on the gas phase optimized structures of the isomers at B3LYP/Lanl2DZ level. Calculation of the natural charges on both the metal atom and the ligands made it possible to understand the global charge transfer from ligands to the metal and vice versa and the contributions of each ligand to this charge transfer. Moreover, the calculation of NBOs, the analysis Donor-acceptor interactions between the NBOs of the metals and ligands made it possible to evaluate the relative σ-donor and π-acceptor character of each ligand in all the isomers of the complexes. It is important to recall that the optimized geometries of the α-M, γ-M, δ-M and ε-M isomers have a C_2 symmetry which makes the charges carried by both Azpy ligands on the one hand and by both chlorine atoms on the other hand identical. The natural charges carried by the metal atoms (Fe, Ru and Os) and each ligand in all the isomers of the complexes at the ground state are given in Table 5.

In Table 5, the Azpy ligands carry positive charges while the chloride ligands carry negative charges. The charges on the metal atoms vary according to the nature of the atoms and the isomers. Here, the charges on Os are all positive regardless the isomer. However, in Fe and Ru complexes, the metallic charges depend on the *cis* or *trans* positions of the Cl atoms. While in the *cis* isomers (α-M, β-M and ε-M) Fe displays negative charge, Ru charge regarding the same isomers are however positive. Whereas in the *trans* isomers (γ-M and δ-M) both metals change their previous charge signs. The charge values of the elements constituting these complexes indicate their role within the molecule. The chloride ligands are electron donors and the Azpy ligand is an electron acceptor. The metal atom is both a donor and an acceptor. Anyhow, the metal charges remain very low. This result agrees with that found by Gottle et al. [29] in the theoretical study of metal-ligand interactions in isomers of the $[Ru(bpy)_2(DMSO)_2]^{2+}$ complex by the NBO method. According to Bamba et al. [5], the ligand that has the greatest natural charge in the molecule determines the affinity of the molecule to bind to DNA. In the complexes studied, the Azpy has the largest charge. Thus, the isomers of each type of complex were classified according to their ligand's charge. For the $FeCl_2(Azpy)_2$ isomers, we have the following order: QL (ε-Fe)> QL (α-Fe)> QL (γ- Fe)> QL (β-Fe)> QL (δ- Fe). As for the isomers of $RuCl_2(Azpy)_2$ and $OsCl_2(Azpy)_2$ complexes, we have respectively the following rankings: QL (δ-Ru)> QL (γ-Ru)> QL (ε-Ru)> QL (α-Ru) > QL (β-Ru) and QL (δ-Os)> QL (ε-Os)> QL (α-Os)> QL (γ-Os)> QL (β-Os). These results indicate that the ε-Cl isomers of the $FeCl_2(Azpy)_2$ complexes

and the δ-M isomers of the $RuCl_2(Azpy)_2$ and $OsCl_2(Azpy)_2$ complexes are likely to bind easily to the DNA.

3.3 Anticancer Effect of Azopyridine Complexes

Cancer is a family of illness related to many causes. Each cause can bring about a specific type of cancer. El-Shahawy et al. defined cancer as a mutual transfer of electrons between nucleic acid bases and an electron donor substrate or an electron acceptor, i.e. free radicals, drugs and even certain foods such as grills and fries. According to them, the bases of the nucleic acid generate carcinogenic cells by loss of electrons. In this process of electron transfer, the bases of DNA can act as electron donors. This is the case for the metabolite of Paracetamol in the liver that gives the N-acetyl-P-benzo-Quinone Imine (NAPQI) which has higher electronic affinity to remove an electron from guanine in the nucleus of the liver cell in the absence of glutathione [30]. As a result, the guanine base loses an electron producing a guanine cation that can behave as a free radical. Positive cancer means that the nucleus lacks an electron because of the mutual transfer of electrons. Therefore, it behaves abnormally. This anomaly is related to the fact that electron loss can generate mutations of certain genes that control cell replication. Therefore, this control system being faulty, the cell begins to divide uncontrollably and becomes cancerous. In this work, the guanine cation will be considered as the cancer cell. This type of cancer can be treated with drugs having a spontaneous electron donor character under a certain condition to compensate the electron deficiency. Organometallic complexes, particularly azopyridine complexes, may be potential candidates for this role. The reasons are of various kinds, among which we have the cytotoxicity of these complexes [31, 32, 8, 33]. Moreover, these complexes are photosensitive [21]. Exposed to light, these complexes can emit electrons to fill the electronic deficit of cancer cells. Therefore, it seems important to evaluate the effect of metals in these complexes regarding the characteristics mentioned above.

3.3.1 Effect on cytotoxicity

Table 6 gathers the specific indices of reactivity such as the electronic chemical potential μ which measures the tendency for electrons to escape from a molecule, the absolute chemical hardness η which expresses the resistance of a system to change its number of electrons, electrophilia ω which can be defined as its ability to bind strongly to a nucleophilic partner by electron transfer and nucleophilia N. Recently, Domingo et al. [19] showed that if a molecule is weakly electrophilic, then it is systematically strongly nucleophilic and only true for simple molecules. For instance, captor-donor ethylene (CD) and complex molecules bearing several functional groups can be both good nucleophiles and good electrophiles [19]. Therefore, the nucleophile index cannot be defined as the inverse of the electrophile. Domingo et al. [20] defined nucleophilia as a negative value of the ionization potential of the gas phase (intrinsic), IP, namely, Nu = - IP. So, high values of nucleophilies correspond to low values of ionization potentials and vice versa. Furthermore, Domingo et al. Used the energies (HOMO) obtained by the Kohn-Sham method, N = εHOMO (Nu) - εHOMO (TCE) where tetracyanoethylene (TCE) is the reference of its lowest energy of the HOMO among the series of molecules already explored in the context of organic polar reactions. This index has been successfully validated by available kinetic experimental data of molecules such like amines, diimines, anilines, alcohols, ethers, alkenes, and Π-nucleophiles.

The analysis of the values in this table indicates several trends. The values of the chemical potentials μ show that all these complexes are nucleophiles with chemical potentials μ which vary between -4,46 and -4,25 relatively to the cancerous cells which will act as electron acceptors with a low chemical potential value of -9.02. β-Fe, δ-Ru and δ-Os isomers have the highest values respectively of -4.40; -4.33 and -4.25. Fortunately, these analyses are strengthened by the chemical hardness. Herein, the least resistant compound to the change of the number of electrons are β-Fe, δ-Ru and δ-Os. However, the most resistant for each type of isomer are assumed to be the γ-Fe, β-Ru and β-Os isomers. Besides, the cancer cells indicate the highest resistance with a chemical hardness value of 2.53 $kcal.mol^{-1}$.

The nucleophile index makes it possible to establish a ranking according to the degree of nucleophilia. Thus, for the iron azopyridine complexes, there is the following classification: N (β-Fe)> N (ε-Fe)> N (δ-Fe)> N (α-Fe)> N (γ-Fe). The isomers of ruthenium and osmium have the following rankings: N (δ-Ru)> N (γ-Ru)> N (ε-Ru)> N (β-Ru)> N (α-Ru) and N (δ-Os)> N (γ-Os)> N (ε-Os)> N (β-Os)> N (α-Os). The

negative value of the nucleophilia of cancer cells indicates that these cells can not engage electrons in interaction with other substrates. The electrophilia index indicates that they are the most electrophilic with a value of 16.07 kcal. mol^{-1}. From the foregoing, it can be deduced that the most active complexes are Os isomers. So, substitution of Ru with Os improves cytotoxicity.

3.3.2 Effect on photosensitivity

3.3.2.1 Effect on the absorption of these compounds

Absorption of each complex was performed using TDDFT calculations. These calculations make it possible to evaluate the sensitization capacity of these complexes. First, we proceed to an optimization followed by a calculation of frequency. The TDDFT calculation is performed on the minimum energy geometry. The level chosen for these calculations is the B3LYP / Lanld2Z level. These azopyridine complexes are characterized by two types of electronic transitions $\pi \rightarrow \pi^*$ and $t_{2g} \rightarrow \pi^*$. The transitions $\pi \rightarrow \pi^*$ have high energy and have wavelengths less than 500 nm. These electronic transitions correspond to Ligand to Ligand Charge Transfer (LLCT). Whereas the $t_{2g} \rightarrow \pi^*$ transitions, they correspond to weak energy with their wavelengths beyond 500nm. They are assumed to represent the Metal to the Ligand Charge Transfer (MLCT). Table 7 lists the main transitions of each type, the energy ($kcal.mol^{-1}$), the maximum wavelength (nm), the oscillation force and the life time, the HOMO and LUMO orbitals of these complexes in their excited state. As for Table 8, it gives the percentage composition of the metal atom, the chlorine atoms and the Azpy ligand of the frontier orbitals involved in each transition selected in Table 7.

TDDFT calculations indicate several electronic transitions of these complexes in the excited state. Two of these transitions for each complex have been selected in Table 7 according to the following criteria: the first transition is the most significant of the $\pi \rightarrow \pi^*$ transitions and the second is the most significant of the $t_{2g} \rightarrow \pi^*$ transitions. The most probable transitions of type $\pi \rightarrow \pi^*$ are those resulting from Os isomers. The most intense is that of the γ-Os isomer with a value of the oscillation force of 0.167 $L.M^{-1}.cm^{-1}$. This isomer absorbs at wavelength of 470.68nm. This transition is from the HOMO-3 to LUMO with a percentage of 83%. Actually, HOMO-3 Orbital of γ-Os is composed of 1% Os, 8% Chlorine and 91% Azpy in reference to Table 8. Whereas LUMO consists of 16% Os, 6% Chlorine and 78% Azpy. Therefore, Os atom has very little influence on this transition. In general, the relative proportions of the metals in these $\pi \rightarrow \pi^*$ transitions are relatively small. This indicates that metals have a weak influence on these types of transitions. The other $\pi \rightarrow \pi^*$ transitions regarding Ru and Fe have relatively low intensities. When we observe the composition of the frontier orbitals involved in these transitions in Table 7, it is found that the HOMOs are mainly formed of orbitals from the chlorine atoms and the Azpy ligand and the LUMOs are mainly centered on the Azpy ligand. So, the electronic delocalization takes place from Cl atoms or Azpy to Azpy ligand. Therefore, it can be assumed that these transitions are of LLCT types.

As for the $t_{2g} \rightarrow \pi^*$ transitions, the most intense are also those resulting from Os isomers. However, the energies of these transitions are relatively high except for the δ-Os isomer which has an absorption band in the therapeutic window that comprise the absorption wavelength of 753.36 nm, with a life time of 16.17ns and an oscillation force of 0.064 $L.M^{-1}.cm^{-1}$[34]. This transition is from HOMO-1 to LUMO with 74%. The HOMO-1 orbital of this isomer consists of 36% Os, 31% of Cl and 33% of Azpy. Thus, the largest proportion comes from Os. Therefore, we can admit that osmium strongly influences this transition. The LUMO δ-Os orbital is made up of 9% Os, 3% Cl and 88% Azpy. So, this electronic transfer is directed mainly to the Azpy. Therefore, this transition is of the MLCT type.

Furthermore, for better use of light in Photo Dynamic Therapy PDT, the absorption band of the selected radiation should be far from the absorption bands of the human body's main tissue. In fact, the body components such as proteins, melanin and hemoglobin absorb in the UV and in the visible. For example, the absorption bands of hemoglobin are 280 nm, 410 nm, 540 nm, 580 nm and about 600 nm [34]. Beyond 1000 nm, we have the absorption band of water thereby locating the therapeutic window between 600nm and 1000nm. Knowing that the absorption bands of $\pi \rightarrow \pi^*$ transitions are not in the therapeutic window; this transition series will thus be used only for treatments requiring a low penetration of light. In general, the $t_{2g} \rightarrow \pi^*$ transitions of these complexes can be involved in several therapeutic processes. For each type of

complex, the isomers that provide the best characteristics are ε-Fe, δ-Ru and δ-Os. Besides, the most important contributions to these transitions generally come from metals. Here, Os provides the best contributions. So, osmium is the most suitable metal for ruthenium substitution in the context of improving therapeutic properties.

3.3.2.2 Effect on florescence characteristics

The isomers that provide the best absorption characteristics are selected here for fluorescence study. The emission and absorption spectra of these complexes (ε-Fe, δ-Ru and δ-Os) are represented in Figs. 3, 4 and 5. These spectra indicate a bathochromic effect between the absorption and emission spectra and a hypochromic effect due to charge and energy transfers. This bathochromic effect that we notice is related to the energy losses that corresponds to the internal conversions and the fluorescence phenomenon will take place for high wavelengths [35]. This shift of the absorption and emission bands is crucial for better detection of the fluorescence signal. The charge and energy transfer processes are favored by the presence of chlorine atoms. These photochemical processes inhibit the fluorescence of azopyridine complexes.

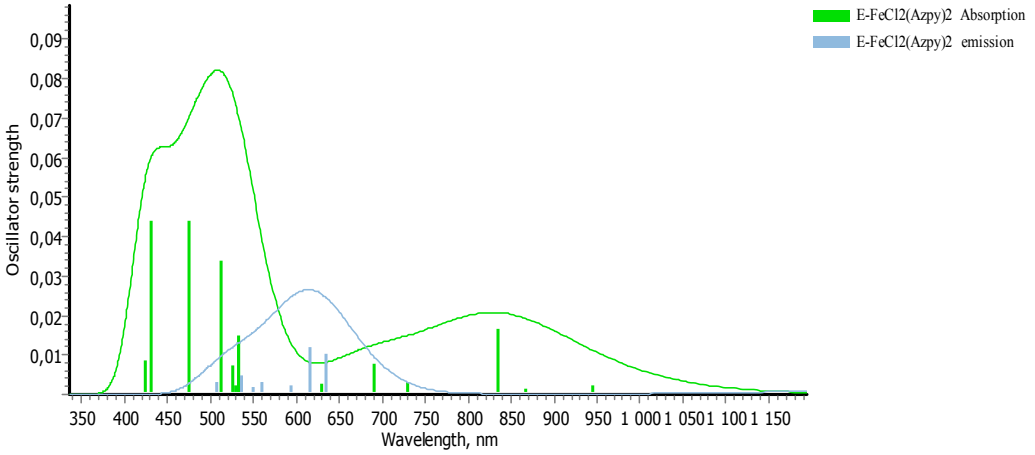

Fig. 3. Emission and absorption spectrum of ε-Fe isomer in the gas phase at B3lyp / LAND2Z level

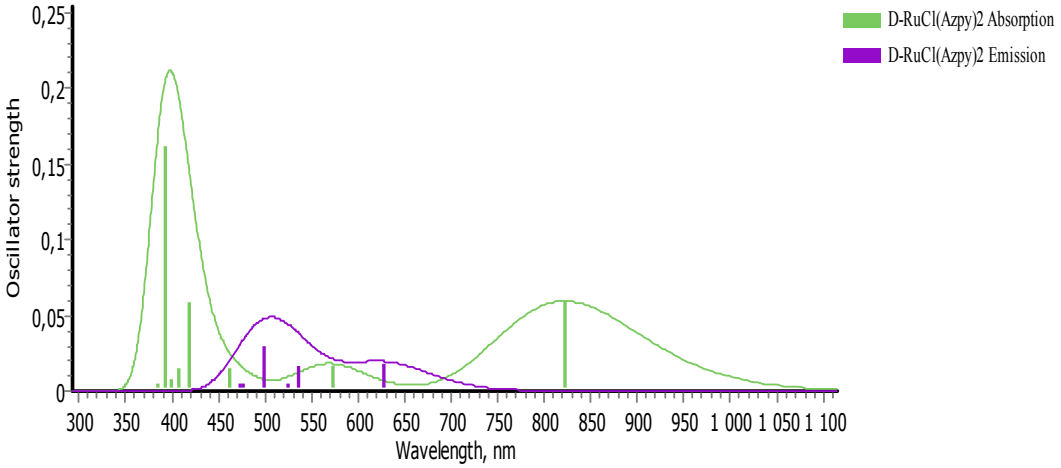

Fig. 4. Emission and absorption spectrum of δ-Ru isomer in the gas phase at B3lyp / LAND2Z level

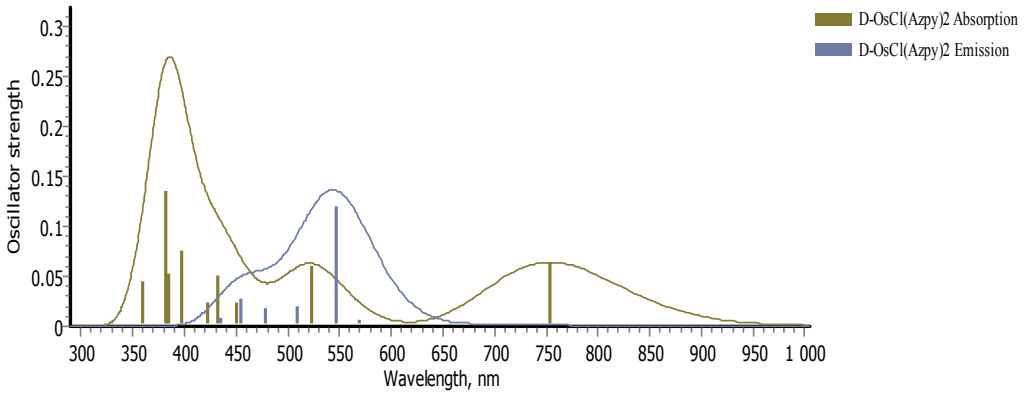

Fig. 5. Absorption and emission spectrum of δ-Os isomer in gas phase at B3lyp / LAND2Z level

Table 9. Fluorescence spectrum parameters, wavelength absorption λ_{Abs}, Stokes shift (Ss), lifetime transition (τ), exciton

Complexes	λ_{Abs} (nm)	Ss (nm)	τ (ns)	E_b (eV)	ε_{max}
ε-Fe	474.49	141.8	639.59	0.19	5200
δ-Ru	393.22	106.03	170.39	-0.69	10000
δ-Os	382.32	164.8	132.72	-1.1	16000

Ss= λ_{max} (émission)-λ_{max}(absorption) $E_b = \Delta E_{L\text{-}H} - E_{flu}$ $E_{flu} = \frac{1\ 240}{\lambda max\ (em)}$

Table 10. Fluorescence spectrum parameters, einstein probability coefficients (A_{if} and B_{if}), dipole moment transition (D_{if}) and oscillation force (F_{if}) of complex Azpy at B3LYP / LANLD2Z level

Isomères	λ_i (nm)	A_{ij} x $10^{-13}s^{-1}$	B_{ij} x 10^{-8} sg^{-1}	D_{ij}	f_{ij}
ε-Fe	833,95	1,563	9,691	0,668	0,0163
δ-Ru	821,66	5,869	1,84	1,27	0,059
δ-Os	753,35	7,534	18,281	1,261	0,0641

To determine the capacity of ε-Fe, δ-Ru and δ-Os complexes to be engaged in a fluorescence process, we evaluated several parameters: First, the absorption wavelength λ_{Abs} that determines the absorption band of the molecule. Secondly, the Stokes shift (Ss) [36] which evaluates the ability for the molecule to distinguish between absorption and emission light. The detection of the fluorescence signal is a function of the value of the Stokes displacement. The larger it is, the better will be the detection of the fluorescence signal. Thirdly, the duration of the transition, also called the life time of the transition (τ) [37]. Fourthly, the energy of attachment of an exciton E_b [38] which is obtained by making the difference between the energy gap and the optical gap. An exciton is a pair comprising an electron and a hole linked by a Coulomb force (electrostatic) and located in the same region of space (orbital overlap). The exciton is formed when an electron passes from the HOMO band to the LUMO band and stays tied to the hole it left behind. It is a quasi-neutral particle that is treated as an hydrogenoid system and determines several optical and optoelectronic properties of the materials [39]. Fifth, the extinction coefficient which is proportional to the intensity of the light emitted. In the absence of a phenomenon that can compete with the fluorescence process, the fluorescence intensity will so increase that the molar absorption coefficient will be higher for a given incident light intensity [37].

Table 9 indicates that ε-Fe has the absorption band having the lowest energy with 474.49 nm as a value of λ_{Abs}. However, δ-Os provides the best fluorescence characteristics. This isomer best distinguishes the light emitted and the light absorbed. This is observed by the value of its stokes displacement which is 164.8 nm. It has the shortest life time estimated at 132.72 ns. This

enhances fluorescence activity and minimizes other forms of energy conversion [39]. It has the lowest attachment energy of excitons. This improves its ability to emit photons and this is confirmed by its molar extinction coefficient which is of the order of 16000. All these metal complexes have a conventional life time comprised between 10^{-10} to 10^{-7} s [36]. Besides, ε-Fe isomer has the longest life time of 639.59 ns. This indicates that in this complex we have a facility of transfer of energy and electrons [39]. Moreover, the analysis of the transitions giving rise to this fluorescence has been characterized by the Einstein parameters. These parameters are recorded in Table 10. The spontaneous emission probability coefficient and the spontaneous absorption probability coefficient. Two parameters are added to the wavelength at which these transitions occur, the oscillation force and the dipole moment of these transitions.

The parameters in Table 10 confirm the performance of δ-Os as It has the highest values. This isomer possesses the most probable emission and absorption with spontaneous emission probability coefficients A_{if} and spontaneous absorption coefficients B_{ij} respectively 7.534 10^{-13} s^{-1} and 18.281sg^{-1}. The dipole moments of transition are arranged in the order D_{ij} (δ-Ru)> D_{ij} (δ-Os)> D_{ij} (ε-Fe). As for the oscillating forces, we have the following order: f_{ij} (δ-Os)>f_{ij} (δ-Ru)>f_{ij} (δ-Os). The results in Tables 9 and 10 indicate that the best fluorophore is the δ-Os isomer [40]. Thus, the substitution of ruthenium by Osmium in the azopyridine complexes increases the fluorescence.

4. CONCLUSIONS

The theoretical exploration of the azopyridine metal complexes such as the α-, β-, γ-, δ-, ε-MCl_2 $(Azpy)_2$ isomers with M = Fe, Os and Ru was carried out in this work with the DFT and TDDFT methods. It showed that the presence of metal within these complexes played a crucial role. The structural analysis carried out on these complexes revealed that all the bonds of MX (with X = Cl, N_2, N_{Py}) underwent an increasing elongation from the iron to the osmium passing through ruthenium. Furthermore, Reactivity, stability, and solubility in organic solvents also evolve following the same trend. Whereas the evaluation of the transitions of the excited states indicates that the second absorption bands of all the isomers were in the therapeutic window except for osmium isomers of which only δ-Os fulfills this condition. This analysis indicates that these azopyridine complexes could be used in photodynamic therapy. Above all, it can be assumed that the activity of azopyridine Ru complexes can be increased by replacing Ru by Os, namely by using δ-$OsCl_2(Azpy)_2$.

COMPETING INTERESTS

Authors have declared that no competing interests exist.

RÉFÉRENCES

1. Torre L, Bray F, Siegel R, Ferlay J, Lortet-Tieulent J, Jemal A. Global cancer statistics 2012.CA: A Cancer Journal for Clinicians. 2015;65:87-108.
2. Sun C, Li Y, Song P, Ma F. An experimental and theoretical investigation of the electronic structures and photoelectrical properties of ethyl red and carminic acid for DSSC application. Materiels. 2016; 9:813.
3. Sava BAG. NAMI-A. Influence of chemical stability on the activity of the anti metastasis ruthenium compound. Eur. J. Cancer. 2002;38 :427–435.
4. Bergamo A. Modulation of the metastatic progression of breast cancer with an organometallic ruthenium compound. Int. J. Oncol. 2008;33:1281–1289.
5. Bamba K, Patrice OW, Nobel NK, Ziao N. SARs investigation of α-, β-, γ-, δ-, ε-RuCl2(Azpy)2 complexes as Antitumor drugs. Computational Chemistry. 2015;4: 1-10.
6. Krause RA, Krause K. Chemistry of bipyridyl-like ligands. Isomeric complexes of ruthenium(II) with 2-(phenylazo)pyridine, Inorg. Chem. 1980;19:2600-2603.
7. Velders AH, Kooijman H, Spek AL, Haasnoot JG, de Vos D, Reedijk J. Inorg. Chem. 2000;39:2966-2967.
8. Hotze GA, Casper ES, Vos D, Kooijma H, Spek LA, Flamigni A, Bacac M, Sava G, Haasnoot GJ, Reedijk J. Structure-dependent *in vitro* cytotoxicity of the isomeric complexes [Ru(L)2Cl2] (L=o-tolylazopyidine and 4- methyl-2-phenylphenylazopyridine) in comparison to [Ru(azpy)2Cl2]. J. Biol. Inorg. Chem. 2004; 9:354–364.
9. Nobel NK, Ouattara WP, Bamba K, Ziao N. Theoretical calculation of influence of halogen atoms (F, Cl, Br, I) on arylazo-pyridine (Azpy) ruthenium complexes behaving as photo sensitizers by DFT

method. International Journal of Advanced Chemistry. 2018;6:67-73.
10. Frisch M, Trucks G, Schlegel H, Scuseria G, Robb M, Cheeseman J, Scalmani G, Barone V, Mennucci B, Petersson G, Nakatsuji H, Caricato M, Li X, Hada M, Ehara M, Toyota K, Fukuda R, Hasegawa J, Hratchian HP, Izmaylov AF, Bloino J, Zheng G, Sonnenberg JL, Hada M, et al. (Gaussian, Inc., Pittsburgh, PA); 1995.
11. Becke AD. A new mixing of Hartree–Fock and local density-functional theories, J. Chem. Phys. 1993;98:1372.
12. Görling A. Density-functional theory for excited states. Phys. Rev. A. 1996;54: 3912.
13. Foresman J, Frisch AE. Exploring chemistry with electronic structure methods. Second ed. Gaussian Inc. Pittsburgh, PA; 1996.
14. Hohenberg P, Kohn W. Inhomogeneous electron gas, Phys. Rev. B. 1964;136:864.
15. Hay PJ, Wadt WR. Ab initio effective core potentials for molecular calculations. Potentials for the transition metal atoms Sc to Hg, J. Chem. Phys. 1985;82:270.
16. Wadt WR, Hay PJ. Ab initio effective core potentials for molecular calculations. Potentials for main group elements Na to Bi, J. Chem. Phys. 1985;82:284.
17. Adamo C, Rebolini E, Savin A. l'actualité chimique. Février-mars. 2014;382-383.
18. Juris A, Balzani V, Barigelletti F, Campagna S, Belser P, Zelewsky A. Ru(II) polypyridine complexes: photophysics, photochemistry, eletrochemistry, and chemiluminescence, Coord. Chem. Rev. 1988;84:85.
19. Domingo LR, Aurell M, Perez P, Contreras R. Quantitative characterization of the global electrophilicity power of common diene/dienophile pairs in Diels–Alder reactions. Tetrahedron. 2002;58:4417.
20. Domingo LR, Chamorro E, Perez P, Jaramillo P, Doming LR, Chamorro E, Perez P. Understanding the reactivity of captodative ethylenes in polar cycloaddition reactions. A Theoretical Study, J. Org. Chem. 2008;73:4615.
21. Nobel NK, Bamba K, Patrice OW, Ziao N. NBO population analysis and electronic calculation of four azopyridine ruthenium complexes by DFT method. Computational Chemistry. 2017;5:51-64.
22. Pavita P, prashanth J, Ramu G, Ramesh G, Reddy KM. Synthesis, structural, spectroscopic, anti-cancer and molecular docking studies on novel 2-[(Anthracene-9-ylmethylene)amino]-2-methylpropane-1,3-diol using XRD, FTIR, NMR, UV–Vis spectra and DFT. Journal of Molecular Structure. 2017;1147:406-426.
23. Shriver DF, Atkins P. Inorganic chemistry. 3rd Edition. New York: Oxford University Press; 1999.
24. Lerner D, Balaceanu S, weinberg c, patron jl. computational study of the molecular complexes between 5-HTP with ATP and DHEA. Potential New Drug Resulting from This Complexation. Computational Chemistry. 2015;3:18-22.
25. Fukui K, Yonezawa T, Shingu H. A molecular orbital theory of reactivity in aromatic hydrocarbons. J. Chem. Phys. 1952;20:722.
26. Salem L. Intermolecular orbital theory of the interaction between conjugated systems. I. General theory. J. Am. Chem. Soc. 1968;9:543.
27. Klopman G. Chemical reactivity and the concept of charge- and frontiercontrolled reactions. J. Am. Chem. Soc. 1968;90:223.
28. Daniel R, Rubio M, Manuela M, Luis S. Ab initio determination of the ionization potentials of DNA and RNA nucleobases. the Journal of Chemical Physics. 2006; 125:084302.
29. Göttle A. Mémoire de thèse. Université de TOULOUSE; 2013.
30. El-Shahawy A. DFT cancer energy barrier and spectral studies of aspirin, paracetamol and some analogues. Computational Chemistry. 2014;2:6-17.
31. Wong E, Giandomenico CM. Current status of platinum-based antitumor drugs. Chem. Rev. 1999;99:2451-2466.
32. Velders A, Kooijman H, Spek A, Haasnoot J, De Vos D, Reedijk J. Strong differences in the *in vitro* cytotoxicity of three isomeric dichlorobis (2-Phenylazopyridine) Ruthenium(II) Complexes. Inorganic Chemistry. 2000;39:2966- 2967.
33. Hotze A, Velders A, Ugozzoli F, Biagini-Cingi M, Manotti-Lanfredi A, Haasnoot J, Reedijk J. Synthesis, characterization, and crystal structure of α-[Ru(azpy)2(NO3)2] (azpy =2-(Phenylazo) Pyridine) and the products of its reactions with guanine derivatives. Inorganic Chemistry. 2000;39: 3838-3844.
34. Rodica-Mariana I. Photodynamic therapy (PDT): A photochemical concept with medical applications. Revue Roumaine de Chimie. 2007;52:1093–1102.

35. Caron T. l'ecole nationale superieure de chimie de montpellier. Mémoire de Thèse. 2010;16.
36. Hlel A, Mabrouk A, Chemek M, Ben, Khalifa I, Alimi K. Computational condensed matter. 2015;3:30-40.
37. Lukes V, Aquino A, Lischka H. Theoretical study of vibrational and optical spectra of methylene-bridged oligofluorenes. J. Phys. Chem. A. 2005;109:10232-10238.
38. Françoise P. mémoire de thèse, Université de Montréal. 2013;28.
39. Hachi M, Khattabi SE, Fitri A, Benjelloun A, Benzakour M, Mcharfi M, Hamidi M, Bouachrine M, Mater J. Environ. Sci. 2018; 9:1200-121.
40. Zhang Y, Zhang L, Wang R, Pan X. Theoretical study on the electronic structure and optical properties of carbazole-π-dimesitylborane as bipolar fluorophores for nondoped blue OLEDs. J. Mol. Graph. Model. 2012;34:46–56.

Peer-review history:
The peer review history for this paper can be accessed here:
http://www.sdiarticle3.com/review-history/48832